

Thermal expansion behaviors of $\text{Li}_3\text{AsW}_7\text{O}_{25}$: a case study for comparative Debye temperature for a large polyatomic unit cell

M. Mangir Murshed^[a,b], Pei Zhao^[a], Ashfia Huq^[c], Thorsten M. Gesing^{*[a,b]}

Dedication to Prof Dr. Thomas Schleid in occasion of his 60th birthday

Abstract: The thermal expansion behavior of $\text{Li}_3\text{AsW}_7\text{O}_{25}$ has been studied. The temperature-dependent development of crystal structural parameters was obtained from Rietveld refinement using neutron time of flight powder diffraction data. Modeling of the lattice thermal expansion was carried out using a Grüneisen first-order approximation for the zero-pressure equation of state, where the temperature-dependent vibrational energy was calculated taking the Debye-Einstein-Anharmonicity approach. Temperature-dependent Raman spectra shed light on some selective modes with unusual anharmonicity. Debye temperatures were calculated using three different theoretical approaches, namely, thermal expansion, mean-squared isotropic atomic displacement parameter and heat capacity. Similarities as well as discrepancies between the numerical values obtained from different theoretical approaches are discussed.

Introduction

The vibration of an atom in a given crystalline system primarily depends on its mass, its surroundings, i.e. the strength of chemical bonding with its neighbors and the temperature. Therefore, each atom sitting in a Wyckoff position of a unit cell has its characteristic vibrational amplitude and is most commonly anisotropic in nature even in a cubic system [1]. For true isotropic atomic vibration, the Debye temperature (θ_D) can be extracted from the Debye-Waller factor (DWF) or directly from the mean-squared isotropic atomic displacement parameter (ADP). The early work of Zener [2] showed that the Debye temperature extracted from the heat capacity (θ_{CV}), thermal expansion (θ_{TE}) and mass-weighted mean ADP (θ_{ADP}) for a given crystalline system differ, and sometimes the difference is significant. Therefore, while using θ_D to calculate another physical parameter it is suggested the method be specified. Barron et al. [3] stated that θ_{CV} should differ from Debye temperature calculated from DWF (θ_{DWF}) by only a few percent. Although the Debye model is likely to be valid for cubic monatomic solids, it has frequently been applied to polyatomic crystals, for instance, for extracting θ_{CV} [4], θ_{TE} [5-10] or θ_{ADP} [11,12]. Horning et al. [13] tabulated $\theta_{CV/CP}$ and θ_{DWF} for some

diatomic systems and suggested a correlation $\theta_{CV/CP} = \sqrt{n} \cdot \theta_{DWF}$ (n = number of types of vibrating species/atoms per asymmetric unit) for polyatomic solids. Notably, this correlation is suggested to be valid up to the classical regime, that is, both $\theta_{CV}(T)$ and $\theta_{DWF}(T)$ are assumed to be roughly constant. Herbstein [14] reviewed comparative Debye temperatures extracted from different methods, which were mainly limited to cubic elemental crystal systems. Polyatomic systems have so far been rarely tested to see whether θ_{CV} , θ_{TE} and θ_{ADP} possess similar numerical values. In a polyatomic system, atoms even with similar mass sitting at different Wyckoff positions have different ADPs, thus each atom possesses its characteristic Debye temperature. The mass-weighted θ_{ADP} values can then be compared with those of θ_{CV} or θ_{TE} . Calculation of the temperature-dependent phonon density of states (PDOS) for a polyatomic system is computationally expensive and therefore calculation of characteristic temperatures either from ADPs, thermal expansion, or C_p/C_V , is still of considerable practical use. The focus of the present study is to obtain θ_{ADP} , θ_{TE} and θ_{CV} values for $\text{Li}_3\text{AsW}_7\text{O}_{25}$ and to compare these numerical values. The large unit cell ($Z = 8$; $a = 724.38(3)$ pm; $b = 1008.15(4)$ pm; $c = 4906.16(17)$ pm; $V = 3582.9(2)$ 10⁶pm³ at 300 K) of the compound is comprised of 36 atoms in the asymmetric unit [15]. In the crystal structure of $\text{Li}_3\text{AsW}_7\text{O}_{25}$ there are seven independent tungsten atoms forming a 2.240(1) nm tungsten-oxide block, connected through isolated arsenic tetrahedra to a 3-D framework. Two of the lithium positions are located in the centroid of hexagonal bipyramids and the third one is arranged along the **a**-direction in alternate order with arsenic atoms [15]. It therefore represents a polyatomic crystal system with 288 atoms in the unit cell.

Results

The starting parameters for the Rietveld refinements were taken from the crystal structure of $\text{Li}_3\text{AsW}_7\text{O}_{25}$ [15]. Fits to the neutron TOF powder data for three representative temperatures are shown in figure 1. The quality of the fit confirms the accuracy of the model. Figure 2 shows the temperature-dependent ADPs of four representative atoms (for better clarity) along with the respective model fit. For modeling, ADPs only from the neutron data analyses were considered as the high-quality data allowed for the independent refinement despite the fact that $\text{Li}_3\text{AsW}_7\text{O}_{25}$ is a condensed system of large unit cell. The in-house X-ray powder data could not be refined for independent ADPs without setting constraints, and were excluded for ADP modeling. The fitting model is based on the Debye approach suggested by Lonsdale [1] as in the following expression:

* Prof. Dr. Thorsten M. Gesing

E-mail: gesing@uni-bremen.de

[a] University of Bremen

Solid State Chemical Crystallography

Institute of Inorganic Chemistry and Crystallography

Leobener Strasse 7 /NW2, D-28359 Bremen, Germany

[b] University of Bremen

MAPEX Center for Materials and Processes

Bibliothekstraße 1, D-28359 Bremen, Germany

[c] Chemical and Engineering Materials Division,

Oak Ridge National Laboratory,

Oak Ridge, Tennessee 37831, USA

$$\langle u_i^2 \rangle = U_{iso} = \left[\frac{145.55 T}{m_i \theta_{Di}^2} \varphi \left(\frac{\theta_{Di}}{T} \right) + A_i \right] \quad (1)$$

Where T , m_i , θ_{Di} refer to temperature, atomic mass and Debye temperature, respectively, of a given vibrating species (atom), and

$$\varphi \left(\frac{\theta_{Di}}{T} \right) = \frac{T}{\theta_{Di}} \int_0^{\frac{\theta_{Di}}{T}} \left[\frac{x}{e^x - 1} \right] dx \quad (2)$$

The A_i parameter (equation 1) is related to the temperature-independent ground state energy and static disorder of an atom [18]:

$$A_i = \frac{36.39}{m_i \theta_{Di}} + B_{static} \quad (3)$$

The fitted parameters are given in table 1. Using the mass weighted average of the atomic Debye temperatures (Tab. 1) θ_{ADP} is calculated as 369(4) K.

Table 1. Fitted parameters of the mean-squared isotropic displacement parameters (ADPs) of $\text{Li}_3\text{AsW}_7\text{O}_{25}$ resulting from equation 1 (estimated standard deviations in the last digit are given in the parentheses throughout the paper).

Atom	θ_{Di}/K	B_{static}/pm^2	Atom	θ_{Di}/K	B_{static}/pm^2
W1	209(6)	5(5)	O8	717(13)	27(5)
W2	242(9)	28(5)	O9	602(15)	10(7)
W3	250(11)	9(6)	O10	738(23)	22(6)
W4	246(7)	5(4)	O11	651(18)	4(2)
W5	378(29)	14(5)	O12	794(32)	6(6)
W6	270(10)	9(4)	O13	868(29)	17(4)
W7	221(6)	21(5)	O14	822(33)	10(6)
As1	390(10)	4(3)	O15	722(24)	4(2)
Li1	799(72)	118(32)	O16	802(27)	15(5)
Li2	466(15)	85(33)	O17	593(16)	24(7)
Li3	603(54)	119(56)	O18	822(24)	5(5)
O1	808(30)	46(6)	O19	433(7)	17(8)
O2	501(9)	8(7)	O20	690(13)	20(4)
O3	913(38)	22(5)	O21	887(24)	5(3)
O4	523(10)	40(7)	O22	780(23)	29(5)
O5	613(16)	5(3)	O23	758(16)	20(4)
O6	552(15)	10(8)	O24	878(36)	11(5)
O7	586(13)	2(3)	O25	558(15)	49(8)

The direct and indirect electronic band gaps of $\text{Li}_3\text{AsW}_7\text{O}_{25}$ are 3.40(4) eV and 2.84(3) eV, respectively [15]. Despite the large ADPs and A -factor for the lithium atoms, temperature-dependent diffusion of lithium has not been observed so far. Therefore, the thermal expansion excludes any electronic as well as ionic contribution, and can be purely described using lattice vibrational internal energy. In some recent reports we simulated the thermal expansion of some mullite-type polyatomic materials using the Debye-Einstein-Anharmonicity (DEA) model for Grüneisen first-order [6,8-10] and second-order [7] approximations for the zero-pressure equation of states. For the present study we consider the first-order approximation where the temperature-dependent metric parameter (M) can be expressed as:

$$M(T) = M_0 + \frac{\gamma U(T)}{K_0} \quad (4)$$

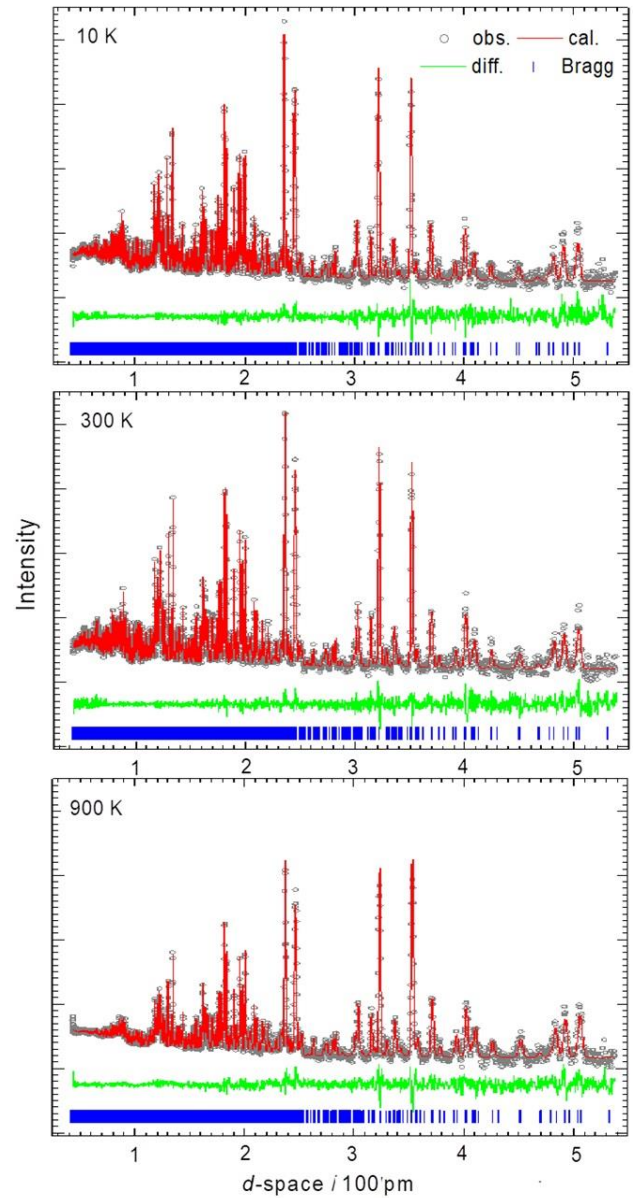


Figure 1. Rietveld plots of neutron powder diffraction data refinements of $\text{Li}_3\text{AsW}_7\text{O}_{25}$ measured at different temperatures. The observed data (empty circles) are given together with the calculated pattern (red line), the difference between observed and calculated data and the position of possible Bragg reflection positions.

M_0 refers to the metric parameter at 0 K, which possesses the zero-point energy. K_0 and γ are the isothermal bulk modulus and the thermodynamic Grüneisen parameter, respectively, and can be treated as $k = \gamma/K_0$ to be the thermoelastic constant. It is well known that calculation of vibrational energy $U(T)$ for polyatomic solids is difficult using a single Debye term in the quasi-harmonic approximation. The parabolic Debye phonon spectrum with a characteristic cut-off frequency cannot truly represent the PDOS. However, for a better description of the PDOS we extended [6-10] equation 4 as follows:

$$M(T) = M_0 + \sum_{i=0}^d k_{Di} U_{Di}(T) + \sum_{j=0}^e k_{Ej} U_{Ej}(T) + \sum_{k=0}^a k_{Ak} U_{Ak}(T) \quad (5)$$

The internal energy $U(T)$ is contributed from the Einstein U_E and Debye U_D along with the low-perturbed anharmonicity U_A [19] with as many as d , e , and a terms for the Debye, Einstein and Anharmonicity contribution, respectively.

The Raman spectrum of the centrosymmetric system shows more or less a single continuum with some modes with unusual Grüneisen parameters (see later), implying that any Einstein term describing an isolated single mode in the PDOS can be excluded from equation 5.

Thus, a further modified model with the following two terms can describe the lattice thermal expansion:

$$U_D(T) = 9Nk_B T \left(\frac{T}{\theta_D}\right)^3 \int_0^{\frac{\theta_D}{T}} \left[\frac{x^3}{\exp(x) - 1} dx \right] \quad (5a)$$

$$U_A(T) = \left[\frac{3Nk_B \hat{a} (\theta_A)^2}{24T \left\{ \exp\left(\frac{\theta_A}{T}\right) - 1 \right\}^3} \left[T \exp\left(\frac{3\theta_A}{T}\right) + 9T \exp\left(\frac{2\theta_A}{T}\right) + 9 \exp\left(\frac{2\theta_A}{T}\right) - 12\theta_A \exp\left(\frac{2\theta_A}{T}\right) - 9T \exp\left(\frac{\theta_A}{T}\right) - 12\theta_A \exp\left(\frac{\theta_A}{T}\right) - T \right] \right] \quad (5b)$$

N refers to the number of atoms per unit cell ($N = 288$), θ_D , and θ_A are the characteristic Debye ($\theta_D = hc\omega_D/k_B T$) and anharmonic temperature. \hat{a} is the anharmonicity parameter. Keeping $\theta_A = \theta_D$ we calculated the anharmonic contribution to the Debye PDOS spectrum. The integral term of the Debye function and the thermal expansion coefficient (TEC, $\alpha_M = \Delta M/M_0 \cdot 1/\Delta T$ [10^{-6}K^{-1}]) are numerically evaluated. The evolution of cell parameters with respect to temperature is shown in figure 3, together with the excellent fit between the model line and the observed data for the metric parameters as well as the TECs. Additionally, the energy contributions of the single terms ($U_D(T)$ and $U_A(T)$) are given to evaluate their contribution.

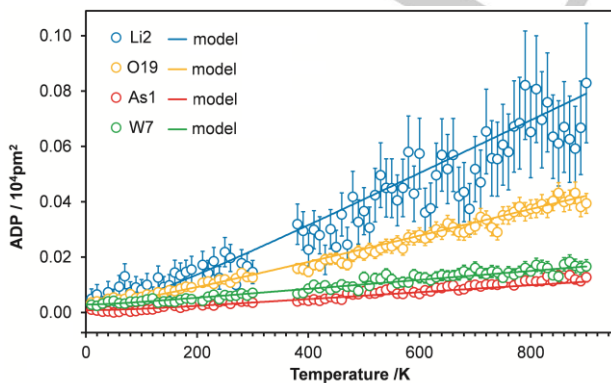


Figure 2. Temperature-dependent isotropic mean-squared atomic displacement parameters (ADPs) of the representative Li-, As-, W- and O-atoms of $\text{Li}_3\text{AsW}_7\text{O}_{25}$ along with the respective Debye model fit.

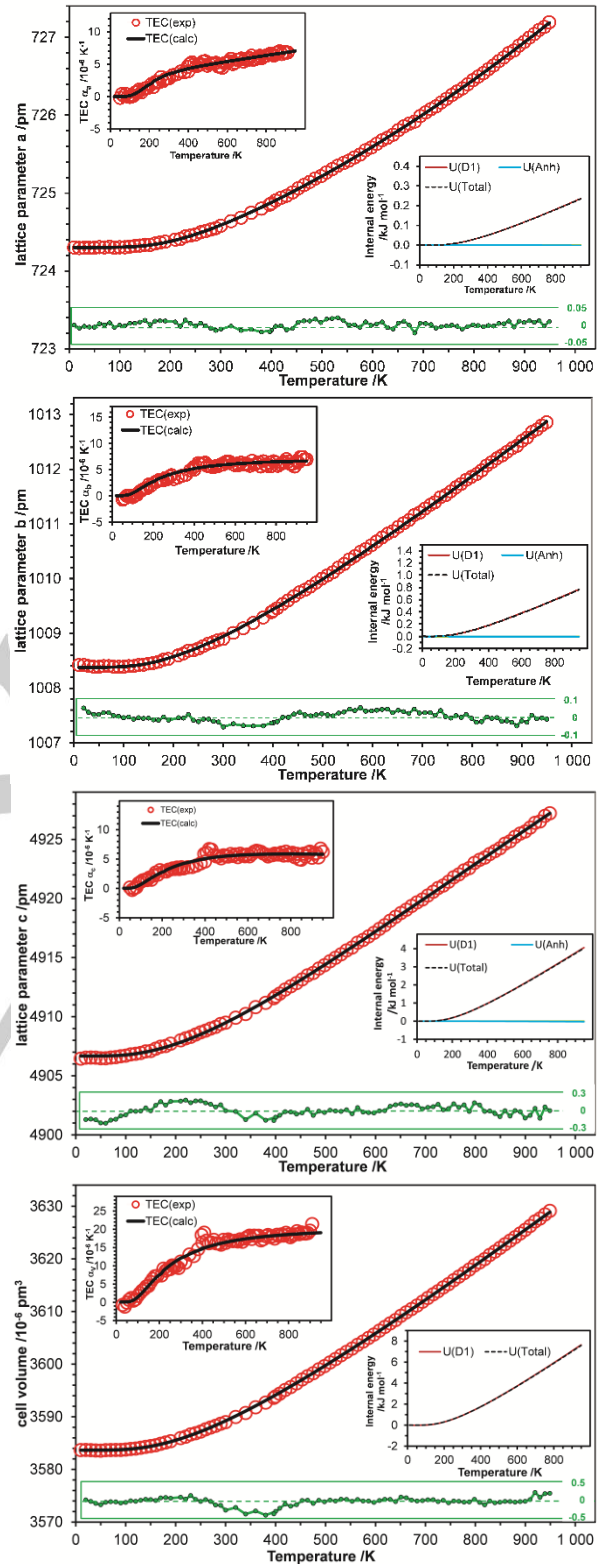


Figure 3. Temperature-dependent metric parameter changes and the respective thermal expansion coefficients (TECs). The solid lines refer to the corresponding DEA models. In the bottom part the difference curve is given with individual scale in pm and 10^{-6}pm^3 for lattice parameters and volume, respectively.

The fitting parameters are given in table 2. Using a single Debye spectrum (model-1) the cell volume can be modeled with an excellent fit ($R^2 = 1$). However, model-1 slightly departs from the observed data above 700 K for all axial metric parameters. Using the Debye model with an anharmonicity term (model-2) the slight deviation between the observed and calculated data diminishes. From the temperature-dependent vibrational energy point of view, the anharmonicity term positively contributes to the a -cell parameter ($\hat{a} = \text{negative}$) and negatively contributes to the b - and c -cell parameter ($\hat{a} = \text{positive}$) (Tab. 2). Using model-1 and model-2, the axial Debye temperatures, in particular for a - and c -cell parameters, significantly differ. However, the averaged Debye temperatures calculated from either of the models lie close to each other (avg. model-1 = 1021(14) K, avg. model-2 = 1020(24) K). These values are close to the value (1013(10) K) calculated from the cell volume.

Table 2. Fitted lattice expansion parameters for $\text{Li}_3\text{AsW}_7\text{O}_{25}$.

M	Model-1 ^a			Model-2 ^a		
	M_0	θ_{TE1}	k_1	θ_{TE2}	k_2	\hat{a}
a	724.30(1)	1267(18)	0.44(1)	1138(20)	0.21(1)	-124(1)
b	1008.39(1)	977(15)	0.61(1)	1058(24)	0.82(1)	30(7)
c	4906.48(5)	819(6)	2.62(2)	863(26)	2.97(2)	15(6)
V	3583.95(5)	1013(10)	6.20(2)	-	-	-

^aLattice parameter a , b and c are given in pm, unit cell volume V in 10^6 pm^3 . θ_{TE1} , and θ_{TE2} refer to Debye temperature [K] calculated from model-1 (Debye-fit) and model-2 (Debye-Anharmonicity fit), respectively. k_1 and k_2 represent the corresponding thermo-elastic parameter [10^{-12} Pa^{-1}] ($k = \text{Grüneisen parameter/Bulk modulus}$). \hat{a} is isochoric anharmonicity parameter [10^{-5} K^{-1}].

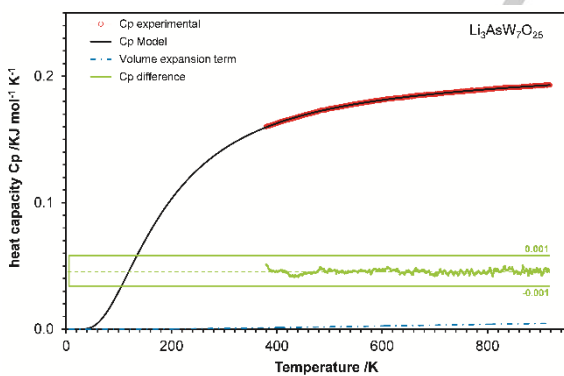


Figure 4. Temperature-dependent heat capacity of $\text{Li}_3\text{AsW}_7\text{O}_{25}$. The difference curve is plotted within the given values on an enlarged scale.

The measured temperature dependence of the heat capacity (C_p) is shown in figure 4 along with the Debye model fit which is valid for C_v only. Although the difference between C_v and C_p is very small and often neglected during the fitting of heat capacity data, the deviations are significant for the determination of the respective Debye temperature. This difference between C_v and C_p is called the volume expansion term $C_{vet} = V(T) \cdot \{\alpha_v(T)\}^2 \cdot T / \kappa_0$ ($V = \text{volume}$, $\alpha_v = \text{thermal expansion coefficient (TEC) of the unit cell volume}$, $T = \text{temperature}$, $\kappa_0 = \text{compressibility} = \kappa_D / \gamma =$

$\text{thermoelastic constant} \cdot \text{Grüneisen parameter}$). Thus $C_{vet} = V(T) \cdot \{\alpha_v(T)\}^2 \cdot T / \kappa_D$. Taking C_{vet} into account $C_p = C_v + C_{vet}$. Using $V(T)$, $\alpha_v(T)$ and κ_D from the DEA fit with $\gamma = 1$, a Debye temperature θ_{Cp} of 717(1) K has been calculated.

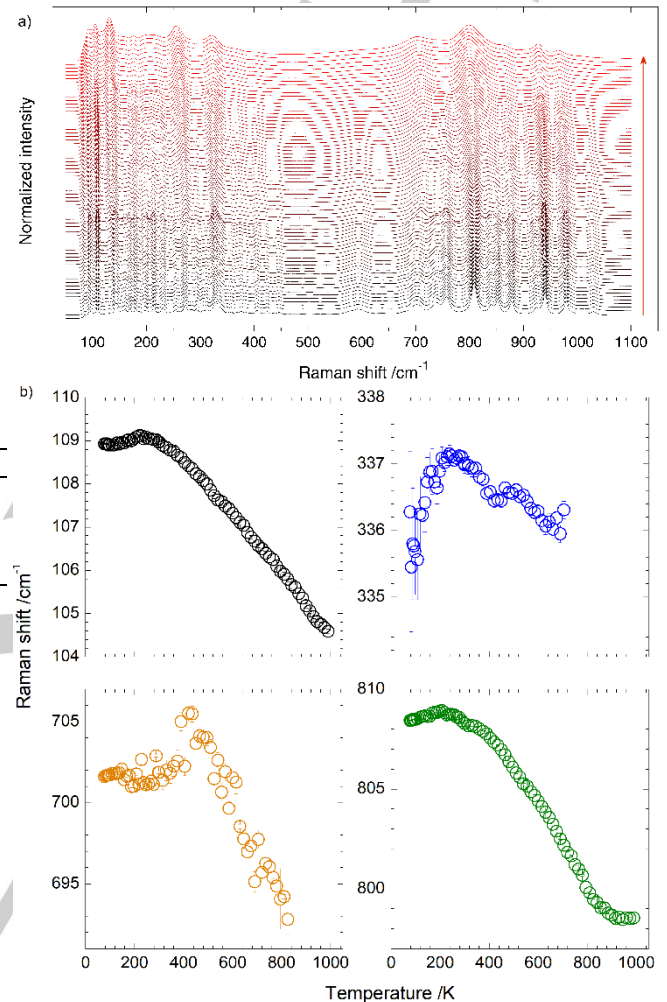


Figure 5. (a) Temperature-dependent Raman spectra of $\text{Li}_3\text{AsW}_7\text{O}_{25}$. The direction of the arrow shows the increase of temperature from 78 K to 900 K. (b) Temperature-dependent anomalies of some selective Raman modes of $\text{Li}_3\text{AsW}_7\text{O}_{25}$.

Using factor group analysis for space group $Pbca$ of $\text{Li}_3\text{AsW}_7\text{O}_{25}$ which contains 288 atoms in the asymmetric unit cell, 432 ($36 \times (3A_g + 3B_1g + 3B_2g + 3B_3g)$) Raman active modes and 321 ($36 \times (3B_1u + 3B_2u + 3B_3u) - \text{acoustic (B1u + B2u + B3u)}$) infrared active modes are expected. However, the spectrum at ambient condition exhibits far less bands in the range 50 cm^{-1} to 1150 cm^{-1} [15]. The temperature-dependent Raman spectra are shown in figure 5. Whereas most of the modes follow the usual monotonic temperature dependency (mode softening and broadening with increasing temperature), some modes show anomalies at different temperature regimes (Fig. 5b). These anomalies correspond to the respective anharmonicity of the

modes, leading to the departure of the Debye model from the observed axial metric data (Fig. 3) at the given temperature. In this regard, the isochoric anharmonicity term of equation 5 (model-2) helps reduce the discrepancy between the model and the observed data.

Discussion

The Debye temperatures calculated from three different approaches ($\theta_{TE1,cell} = 1013(10)$ K, $\theta_{ADP} = 369(4)$ K, $\theta_{CP} = 717(1)$ K) are different. Using the Horning [13] analogy a Debye temperature ($\sqrt{n^*}\theta_{ADP}$) of 738(4) K can be calculated, which lies close to θ_{CP} . The Debye temperature bears significance as a physical constant of any given crystalline system. Thus, the numerical value is expected to be similar within certain accuracy irrespective of the methods used calculate it. Since modeling of C_P data could not be performed at low-temperatures, a comparison between the numerical values cannot be made. Moreover, each calculation approach encounters the Debye approximation differently. Lonsdale [1] particularly emphasized that the vibrational amplitude of a given species should not necessarily be isotropic since the elastic waves can vary in any direction due to the elastic tensor. In the Grüneisen approximation (equation 4), both the Grüneisen parameter and the bulk modulus are assumed to be temperature-independent, whereas in reality, both tensors are sensitive to temperature. Blackman [20] pointed out that a Debye temperature calculated from the heat capacity will not provide accurate information at temperatures higher than $\frac{1}{2}\theta_{CP}$. These discrepancies can be also visible from the respective theoretical approaches. The weighting factors $f(\hbar\omega/k_B T)$ associated with the PDOS for the calculation of ADP, thermal expansion and C_V are as follows [14,21-23]:

$$f_{ADP}\left(\frac{\hbar\omega}{k_B T}\right) = \frac{k_B T}{\hbar\omega} \left[\frac{1}{\exp\left(\frac{k_B T}{\hbar\omega}\right) - 1} + \frac{1}{2} \right] \quad (6)$$

$$f_{TE}\left(\frac{\hbar\omega}{k_B T}\right) = \left[\frac{\frac{\hbar\omega}{k_B T}}{\exp\left(\frac{k_B T}{\hbar\omega}\right) - 1} \right] \quad (7)$$

$$f_{CV}\left(\frac{\hbar\omega}{k_B T}\right) = \left[\frac{\left(\frac{\hbar\omega}{k_B T}\right)^2 \exp\left(\frac{\hbar\omega}{k_B T}\right)}{\left(\exp\left(\frac{k_B T}{\hbar\omega}\right) - 1\right)^2} \right] \quad (8)$$

The weighting factors are shown in figure 6 as functions of both frequency and temperature, leading to different sensitivity to the frequency distribution at different temperatures. It is clear that ADPs are sensitive to low-frequency and, C_V to high frequency for a given characteristic temperature. In comparison, the thermal expansion approach is moderately sensitive to the whole temperature regime. Since the Debye parabolic shape almost mimics the actual PDOS spectrum at low-frequency region, it is reasonable to assume that Debye approximation more accurately fits low-temperate ADPs than the C_V or the

thermal expansion approaches. The Debye elastic approach is the simplest lattice-dynamical model and links between the elasticity and the acoustic phonons close to the zone center. The model has two approximations: (I) the phonon dispersion curves are linear with slopes that provide the elastic coefficients and (II) the bulk and shear moduli are used instead of elastic tensors, thus the shape of the Brillouin zone is assumed to be spherical. The model works well for simple elemental crystals, as the monatomic solids possess only three acoustic modes [14]. However, for a polyatomic solid such as in the present study on $\text{Li}_3\text{AsW}_7\text{O}_{25}$, more crude approximations should be taken into account. For instance, the optic modes are assumed to behave as the acoustic ones, that is, similar frequency distributions

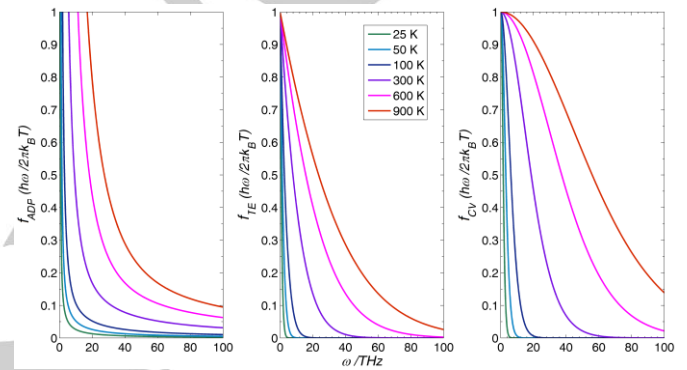


Figure 6. Variation of the weighting factor f_i with frequency and temperature. f_{ADP} , f_{TE} and f_{CV} are the weighting factors multiplied with the PDOS of the respective integrand of the theoretical model for mean-squared isotropic atomic displacement parameter (ADP), thermal expansion (TE) and heat capacity at constant volume (C_V), respectively.

and mode Grüneisen parameters. Since for complex solids the optic phonons dominate the lattice dynamical property, which is significantly different from that of the acoustic phonons, the Debye model eventually breaks down. In other words, in a Debye solid it is assumed that all atoms have a constant proportion to each other, determined by relative masses and numbers of atoms per asymmetric unit, at each frequency within the PDOS. However, in reality, the maximum frequencies for different vibrational species/modes are not the same (Tab. 1). That is, the atomic contributions to the PDOS must localize in the PDOS-spectrum depending on the strength of the chemical bonds within a polyhedral environment. For instance, even though Mg is lighter than Si, its vibrational contributions are seen in the lower frequency region, and those of Si in the higher frequency region of the PDOS of MgSiO_3 perovskite [24]. However, separation of the Raman frequencies associated with the AsO_4 , WO_6 and the LiO_x polyhedra of the large $\text{Li}_3\text{AsW}_7\text{O}_{25}$ system is difficult [15]. For this reason, it is not surprising that the modeling of each metric parameter requires only one Debye continuum. Beside the crude assumptions of the Debye approximation, the need for Debye temperatures is to estimate correlated physical parameters for the polyatomic large systems is still demanding. If any of the site-chemistry of $\text{Li}_3\text{AsW}_7\text{O}_{25}$

changes, Debye temperatures calculated from any of the temperature-dependent parameters may well predict the mechanical properties, melting point [25], thermal conductivity [26], due to the changed chemistry [27]. This study particularly shows that if the frequency spectrum is condensed for a complex large system, the DEA model [5-10] can estimate the Debye temperature with certain accuracy.

Experimental Section

Neutron time of flight powder diffraction data were collected on the high-resolution powder diffractometer, Powgen at the Spallation Neutron Source (SNS), Oak Ridge National Laboratory (ORNL), USA. The low-temperature data were collected in an automated sample changer between 10 K and 300 K with a 10 K step using the center wavelength of 13.3(1) pm for about 25 min at each temperature step. The high-temperature data were collected between 380 K and 900 K with steps of 10 K using the ILL furnace. To fill the temperature gap between 300 K and 380 K, X-ray powder diffraction data were collected on a PANalytical MPD powder diffractometer in Bragg-Brentano geometry equipped with a secondary Ni filter, Cu K $\alpha_{1,2}$ radiation and an X'Celerator detector using a high-temperature chamber HTK 1200N (Anton Paar Co.). Data were collected between 5° and 130° 2 θ with a step width of 0.0167° and a collection time of 45 s/step. Rietveld refinements were performed using the GSAS [16] platform with EXPGUI interface [17]. During the refinement the scale factor, absorption coefficient and two profile shape parameters, lattice parameters, fractional coordinates of the atoms and their displacement parameters were optimized. In table 3 the 300 K lattice parameters obtained here from neutron powder diffraction TOF data are compared to those described in [15] from single crystal data, clearly showing that referring to single crystal data much higher e.s.d.'s are to be considered as evaluated for the data sets. Further details of the crystal structure investigations, including all positional and displacement parameters, may be obtained from FIZ Karlsruhe, 76344 Eggenstein-Leopoldshafen, Germany (fax: (+49)7247-808-666; E-Mail: crysdata@fiz-karlsruhe.de, on quoting the deposition numbers CSD-433919 to CSD-434000. Note, at temperatures between 10 K and 110 K in total 23 of 396 displacement parameters for atom positions W6 (6x), O3 (4x), O8 (1x), O10 (2x) and O22 (10x) became slightly negative, in the fifth digit, during the refinements. The values are close to zero because of the low temperature of the sample during data collection and are not further away from zero as 1 or 1.5 standard deviations. This is within the possibility of mathematical/physical treatment of the data. Therefore, we don't like to manipulate the calculations and kept them as they are.

Table 3. Lattice parameter for Li₃AsW₇O₂₅.

a /pm	b /pm	c /pm	V / 10 ⁶ pm ³	T/K	Ref.*
724.38(3)	1008.15(4)	4906.16(17)	3582.9(2)	RT*	SC [15]
724.58(1)	1008.90(1)	4909.49(6)	3588.97(5)	300	ND
724.30(1)	1008.39(1)	4906.48(5)	3583.95(5)	0	fit

*RT: room-temperature data, SC: single crystal data, ND neutron powder diffraction data evaluated for this work, fit: DEA model fit results, see table 2.

Raman spectra were recorded on a Horiba LabRam Aramis spectrometer equipped with a laser excitation wavelength of 633 nm. Data were recorded using a grating of 1800 grooves/mm in the Raman shift range between 50 cm⁻¹ and 1100 cm⁻¹. The samples were pressed into powder pellets. For the temperature-dependent measurements, the pellets were placed separately in a Linkam cooling (THMS600) and heating (TS1500) stage for the range of 78 K to 900 K.

The heat capacity (C_p) measurements were carried out using approx. 90 mg sample on a Netzsch STA 449C analyzer in the IKZ Berlin laboratory over the temperature range of 313 and 923 K with a heating speed of 20 K/min in 1 K increment slices. Due to known systematic instrument effects at lower temperature, data have been cut below 380 K and were not further used for the determination of the Debye temperature.

Acknowledgements

MMM gratefully acknowledges the University of Bremen for financial support. PZ thanks the China Scholarship Council to carry out this work through a fellowship. The research at Spallation Neutron Source was sponsored by the Scientific User Facilities Division, Office of Basic Energy Sciences, U.S. Department of Energy. We also would like to thank Dr. Detlef Klimm (Institut für Kristallzüchtung, Berlin, Germany) for the collection of the C_p data.

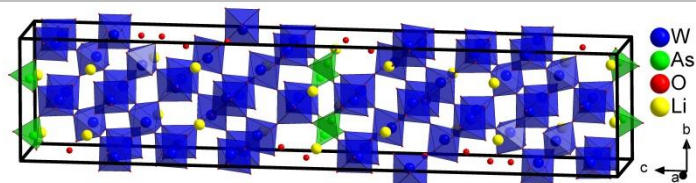
Keywords: Lithium-arsenotungstate • neutron diffraction • Raman spectroscopy • thermal expansion • Debye temperature

- [1] K. Lonsdale, *Acta Crystallogr.* **1948**, 1, 142.
- [2] C. Zener, *Phys. Rev.* **1936**, 49, 122.
- [3] T.H.K. Barron, A.J. Leadbetter, J. Morrison, L.S. Salter, *Acta Crystallogr.* **1966**, 20, 125.
- [4] B. Hildmann, H. Schneider, *Evaluation* **2004**, 34, 227.
- [5] M.M. Murshed, M. Šehović, M. Fischer, A. Senyshyn, H. Schneider, T.M. Gesing, *J. Am. Ceram. Soc.* **2017**, 100, 5259.
- [6] M.M. Murshed, P. Zhao, M. Fischer, A. Huq, E. V. Alekseev, T.M. Gesing, *Mater. Res. Bull.* **2016**, 84, 273.
- [7] M. Mangir Murshed, C.B. Mendive, M. Curti, M. Šehović, A. Friedrich, M. Fischer, T.M. Gesing, *J. Solid State Chem.* **2015**, 229, 87.
- [8] M.M. Murshed, C.B. Mendive, M. Curti, G. Nénert, P.E. Kalita, K. Lipinska, A.L. Cornelius, A. Huq, T.M. Gesing, *Mater. Res. Bull.* **2014**, 59, 170.
- [9] M.M. Murshed, T.M. Gesing, *Mater. Res. Bull.* **2013**, 48, 3284.
- [10] T.M. Gesing, C.B. Mendive, M. Curti, D. Hansmann, G. Nénert, P.E. Kalita, K.E. Lipinska, A. Huq, A.L. Cornelius, M.M. Murshed, *Z. Kristallogr.* **2013**, 288, 532.
- [11] D.M. Trots, A. Senyshyn, L. Vasylechko, R. Niewa, T. Vad, V.B. Mikhailik, H. Kraus, *J. Phys. Condens. Matter* **2009**, 21, 325402.
- [12] A. Senyshyn, H. Boysen, R. Niewa, J. Bany, M. Kinka, Y. Burak, V. Adamiv, F. Izumi, I. Chumak, H. Fuess, *J. Phys. D. Appl. Phys.* **2012**, 45, 175305.
- [13] R.D. Horing, J.-L. Staudenmann, *Acta Crystallogr. Sect. A Found. Crystallogr.* **1988**, 44, 136.
- [14] F.H. Herbstein, *Adv. Phys.* **1961**, 10, 313.
- [15] P. Zhao, M. Mangir Murshed, A. Huq, H.K. Grossmann, L. Mädlar, E. V. Alekseev, T.M. Gesing, *J. Solid State Chem.* **2015**, 226, 81.
- [16] A.C. Larson, R.B. Von Dreele, *Structure* **2004**, 748, 86.
- [17] B.H. Toby, *J. Appl. Crystallogr.* **2001**, 34, 210.
- [18] D.N. Argyriou, *J. Appl. Crystallogr.* **1994**, 27, 155.
- [19] A.R. Oganov, P.I. Dorogokupets, *J. Phys. Condens. Matter* **2004**, 16, 1351.
- [20] M. Blackman, in: *Handb. Der Phys.* VII, Springer, Berlin, **1955**, p. 325.
- [21] M. Blackman, *Proc. Camb. Philol. Soc.* **1937**, 33, 380.
- [22] G. Eckold, in: *Int. Tables Crystallogr.*, International Union of Crystallography, **2006**, pp. 266–293.
- [23] M.T. Dove, *Structure and Dynamics, an Atomic View of Materials*, Oxford University Press, **1993**.
- [24] A.R. Oganov, J.P. Brodholt, G.D. Price, *Phys. Earth Planet. Inter.* **2000**,

- 122, 277.
- [25] W. Nernst, F.A. Lindemann, *Z. Electrochem. Angew. Phys. Chem.* **1911**, 17, 817.
- [26] M. Beekmann, A. VanderGraaff, *J. Appl. Phys.* **2017**, 121, 205105.
- [27] K. Hoffmann, M.M. Murshed, R.X. Fischer, H. Schneider, T.M. Gesing, *Z. Kristallogr.* **2014**, 229, 699.

WILEY-VCH

FULL PAPER



The thermal expansion behavior of $\text{Li}_3\text{AsW}_7\text{O}_{25}$ has been studied. Debye temperatures are calculated from thermal expansion using the DEA model, mean-squared isotropic atomic displacement parameter and heat capacity. Similarities as well as discrepancies between the numerical values obtained from different theoretical approaches are discussed.

*M. Mangir Murshed, Pei Zhao, Ashfia Huq, Thorsten M. Gesing**

1 – 6

Thermal expansion behaviors of $\text{Li}_3\text{AsW}_7\text{O}_{25}$: a case study for comparative Debye temperature for a large polyatomic unit cell

Additional Author information for the electronic version of the article.

Author: Prof. Dr. Thorsten M. Gesing, ORCID identifier 0000-0002-4119-2219
Author: PD Dr. M. Mangir Murshed, ORCID identifier 0000-0002-9063-372X
Author: Dr. Pei Zhao, ORCID identifier 0000-0002-8179-1291.
Author: Dr. Ashfia Huq, ORCID identifier 0000-0002-8445-9649

WILEY-VCH
